



Inorganic/whole-cell biohybrid photocatalyst for highly efficient hydrogen production from water

Yuki Honda ^{a,*}, Motonori Watanabe ^a, Hidehisa Hagiwara ^{a,b}, Shintaro Ida ^{a,b}, Tatsumi Ishihara ^{a,b}

^a International Institute for Carbon-Neutral Energy Research, Kyushu University, 744 Motooka, Nishi-ku, Fukuoka 819-0395, Japan

^b Department of Applied Chemistry, Faculty of Engineering, Kyushu University, 744 Motooka, Nishi-ku, Fukuoka 819-0395, Japan

ARTICLE INFO

Article history:

Received 16 February 2017
Received in revised form 1 April 2017
Accepted 5 April 2017
Available online 7 April 2017

Keywords:

[FeFe]-hydrogenase
Inorganic-bio hybrid
Photocatalysis
Water splitting
Whole-cell biocatalyst

ABSTRACT

To obtain a clean hydrogen production system, we have developed an inorganic-bio hybrid photocatalyst system based on the combination of anatase TiO_2 , methylviologen (MV) as an electron mediator, and a whole-cell biocatalyst consisting of [FeFe]-hydrogenase and maturase gene-harboring recombinant *Escherichia coli*; however, the apparent quantum yield at 300 nm (AQY₃₀₀) for hydrogen production was low (0.3%). The system consists of a two-step reaction: (1) photocatalytic MV reduction by TiO_2 , and (2) hydrogen production with reduced MV using a biocatalyst. The enhancement of step 1 under biocatalyst-friendly conditions was investigated in an attempt to further improve the reaction efficiency. Among the condition tested, the use of 100 mM Tris-HCl (pH 7), 150 mM NaCl, and 5% (v/v) glycerol with P-25 TiO_2 especially enhanced the step 1 reaction by a 300-fold increase in the MV reduction rate compared with previously tested reaction condition (100 mM Tris-HCl (pH 7), 150 mM NaCl, 5% (v/v) glycerol, and 100 mM ascorbate with anatase TiO_2). Under the enhanced step 1 reaction, AQY₃₀₀ and AQY₃₅₀ for photocatalytic MV reduction reached 60.8% and 52.2%, respectively. The enhanced step 1 reaction thus significantly improved the overall photocatalytic hydrogen productivity of the hybrid system and AQY₃₀₀ and AQY₃₅₀ reached 26.4% and 31.2%, respectively. The inorganic-whole-cell biohybrid system can therefore provide noble metal-free, efficient, and clean hydrogen production.

© 2017 Elsevier B.V. All rights reserved.

1. Introduction

Hydrogen formed via an environmentally friendly process is regarded as a promising energy carrier to achieve sustainable energy generation. In particular, photocatalytic water splitting using solar energy has attracted significant interest because such a system is capable of hydrogen production without the formation of CO_2 and without other supplemental energy requirements [1–3]. With an aim to develop an efficient system for hydrogen production, we have focused on an inorganic-bio hybrid photocatalyst system that combines an inorganic semiconductor and a biocatalyst. In the inorganic-bio hybrid system, the inorganic semiconductor is used as a catalyst to capture and convert light energy into chemical energy, and the biocatalyst is used for the efficient formation of hydrogen. Some inorganic-bio hybrid pho-

tocatalyst systems for hydrogen production have been developed where purified hydrogenase is employed as a biocatalyst [4] because hydrogenases are known to be highly efficient hydrogen-forming biocatalysts [5,6]. For example, some research groups have developed an inorganic-bio hybrid photocatalyst system through combinations of TiO_2 with bacterial hydrogenase [7,8] and archaeal [NiFe]-hydrogenase [9], dye-sensitized TiO_2 or TiO_2 -coated *p*-Si photocathode with [NiFeSe]-hydrogenase [10–12], nitrogen-doped TiO_2 with [FeFe]-hydrogenase [13], and CdTe or CdS with recombinant clostridial [FeFe]-hydrogenase [14–16]. These systems have demonstrated the potential of inorganic-bio hybrid systems for hydrogen production; however, the stability of the enzyme and the time-consumption and costly manipulations involved (e.g., cell disruption and protein purification steps) have hampered their practical application.

To overcome these problems, we have employed a whole-cell biocatalyst instead of purified hydrogenases, and developed a new inorganic-bio hybrid photocatalyst system that combines anatase TiO_2 , methylviologen (MV) as an electron mediator, and a whole-cell biocatalyst that consists of recombinant *Escherichia coli* that harbors genes to encode clostridial [FeFe]-hydrogenase and mat-

Abbreviations: AA, ascorbic acid; AQY, apparent quantum yield; CB, conduction band; GC, gas chromatography; Gly, glycerol; MV, methylviologen; VB, valence band.

* Corresponding author.

E-mail address: yhonda@i2cner.kyushu-u.ac.jp (Y. Honda).

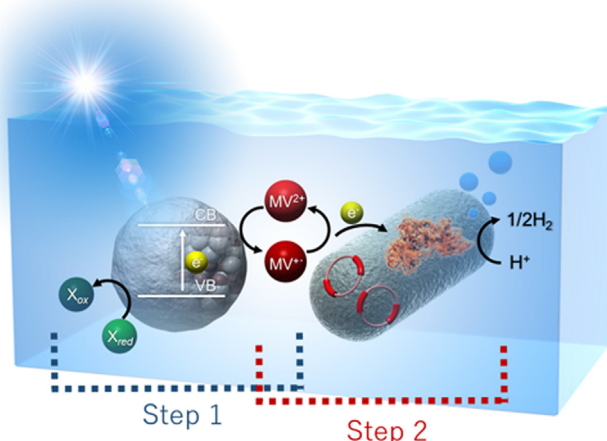


Fig. 1. Photocatalytic hydrogen production system using the combination of an inorganic semiconductor, an electron mediator, and a whole-cell biocatalyst (recombinant *E. coli*). The system consists of a two-step reaction: (1) photocatalytic methylviologen (MV) reduction by an inorganic semiconductor, and (2) hydrogen production by the whole-cell biocatalyst from reduced MV. Recombinant *E. coli* BL21(DE3)/pEHydEA + pCHydFG was used as the hydrogen-forming biocatalyst.

urase (Fig. 1) [17]. The whole-cell biocatalyst is easily obtained by simply harvesting cells from a culture, and possesses greater stability than that of purified hydrogenase. Our previous research demonstrated that the inorganic semiconductor/whole-cell biocatalyst hybrid system is capable of hydrogen production under light irradiation, without the need for accompanying cell lysis or disruption during the photocatalytic reaction [17]. The reaction consists of two steps: (1) photocatalytic MV reduction by TiO_2 , and (2) hydrogen production from reduced MV using the whole-cell biocatalyst (Fig. 1). The system can produce hydrogen under light irradiation; however, the apparent quantum yield (AQY, represented as $100 \times (2 \times \text{number of hydrogen molecules formed}) / (\text{number of incident photons})^{-1}$) achieved under monochromatic light irradiation at 300 nm was low ($\text{AQY}_{300} = 0.3\%$) [17]. Therefore, an improvement in the AQY is required for practical application of this semiconductor/whole-cell system. In the previous study, recombinant *E. coli* BL21(DE3)/pEHydEA + pCHydFG, which harbors [FeFe]-hydrogenase and maturase genes (*hydA*, *hydE*, *hydF*, and *hydG*) from *Clostridium acetobutylicum* NBRC 13948, was constructed, and demonstrated that as the recombinant *E. coli* whole-cell biocatalyst produced hydrogen from 5 mM of reduced MV with an activity of approximately $0.7 \mu\text{mol-H}_2 \text{ min}^{-1} (\text{mg-wet-cell})^{-1}$ [17]. This whole-cell reaction corresponds to step 2 shown in Fig. 1. However, the combination of anatase TiO_2 , MV, and the whole-cell recombinant *E. coli* (Anatase/MV/Whole-cell) can produce hydrogen under light irradiation with a hydrogen production rate of ca. $6 \times 10^{-3} \mu\text{mol-H}_2 \text{ min}^{-1} (\text{mg-wet-cell})^{-1}$, which is normalized according to the weight of the whole-cell biocatalyst under the previously reported conditions [17]. Thus, in the previous system, less than 1% of the capacity of the step 2 reaction by recombinant *E. coli* is used, which suggests that hydrogen production could be improved by a more efficient rate of supply of the reduced in step 1. Therefore, the enhancement of step 1 (MV reduction) is the target for improvement of the photocatalytic hydrogen productivity of the entire system.

The objective of this study was to improve the photocatalytic hydrogen productivity and AQY of the novel inorganic-bio hybrid photocatalyst system by the enhancement of MV reduction by an inorganic semiconductor, which is a part of the system reaction (step 1). The inorganic-bio hybrid photocatalyst system was improved by conducting the following experiments: 1) screening

of conditions for efficient photocatalytic MV reduction, 2) screening of inorganic semiconductor photocatalysts, and 3) application of enhanced MV reduction to photocatalytic hydrogen production with the inorganic-bio hybrid system. Furthermore, the efficiencies and AQYs for each step, photocatalytic MV reduction and hydrogen production, were investigated.

2. Experimental section

2.1. Materials

Inorganic semiconductors, anatase TiO_2 (Wako Pure Chemical Industries, Ltd.), rutile TiO_2 (STR-100N, Sakai Chemical Industry Co., Ltd.), P-25 TiO_2 (Nippon Aerosil Co., Ltd.), ZrO_2 (Wako), Nb_2O_5 (Kishida Chemical Co., Ltd.), Ta_2O_5 (Wako), and ZnO (Kojundo Chemical Laboratory Co., Ltd.) were tested as-received from the supplier and without further treatment. $\text{KTa}(\text{Zr})\text{O}_3$, Ga_2O_3 and GaN:ZnO were also prepared in our laboratory according to the previously described methods ($\text{KTa}(\text{Zr})\text{O}_3$ [18], Ga_2O_3 [19], and GaN:ZnO [20,21]). 2-amino-2-hydroxymethyl-1,3-propandiol (Tris; Nacalai Tesque, Inc.), HCl (Wako), NaCl (Wako), L-ascorbic acid (Wako), glycerol (Kishida Chemical) and 1,1'-dimethyl-4,4'-bipyridium dichloride (methylviologen, MV; Tokyo Chemical Industry Co., Ltd.) were purchased from commercial manufacturers. The whole-cell biocatalyst of *E. coli* BL21(DE3)/pEHydEA + pCHydFG was prepared according to a previously reported method [17]. Ultrapure water was used for all experiments and reaction solution preparations.

2.2. Photocatalytic MV reduction

Photocatalytic MV reduction was conducted using a $10 \text{ mm} \times 10 \text{ mm}$ quartz cuvette with a screw cap and a light source (300 W Xe lamp). The reaction mixture consisted of 1 mg of each inorganic semiconductor, 3 mL of the reaction solution, and 5 mM of MV in the quartz cuvette with a stirring bar. Oxygen was removed by bubbling nitrogen gas into the mixture for 20 min. The reaction was initiated by light irradiation. Absorption spectra were measured using an absorbance microplate reader with the quartz cuvette measurement option (SH-1000Lab, Corona Electric Co., Ltd., Japan) after the quartz cuvette was centrifuged (1000g for 1 min) to remove the effects of inorganic semiconductor powder diffusion on the absorbance spectra. The amount of reduced MV ($\text{MV}^{\bullet-}$) formed was calculated from the absorbance at 605 nm using a molar conversion coefficient, ϵ , of $1.3 \times 10^4 \text{ M}^{-1} \text{ cm}^{-1}$ [22].

2.3. Photocatalytic hydrogen production

Photocatalytic hydrogen production was performed using the combination of an inorganic semiconductor, an electron mediator, and the whole-cell biocatalyst. The reaction was performed using a closed gas circulation system with Ar gas as the circulating carrier with a 300 W Xe lamp as the external light source. The reaction mixture consisted of 20 mL of 100 mM Tris-HCl (pH 7), 150 mM NaCl, 5% (v/v) glycerol, 5 mM MV, 50 mg of the inorganic semiconductor powder, and 0.1 g-wet-cell of the whole-cell biocatalyst. The reaction mixture was prepared in a glovebox (97% nitrogen and 3% hydrogen atmosphere, oxygen <1 ppm). After the quartz reaction cell was connected to the gas circulation system, the atmosphere of the system was evacuated and replaced with Ar gas to remove the nitrogen and hydrogen from the glovebox atmosphere. Reaction without light irradiation was conducted for 1 h to verify that there was no gas leakage. The amount of hydrogen formed was analyzed using gas chromatography with thermal conductivity detector (GC; GC-8A, Shimadzu Corp., Japan, equipped with an integrator C-R6A (Shimadzu Corp.) and a Molecular Sieve 5A column (GL Sciences

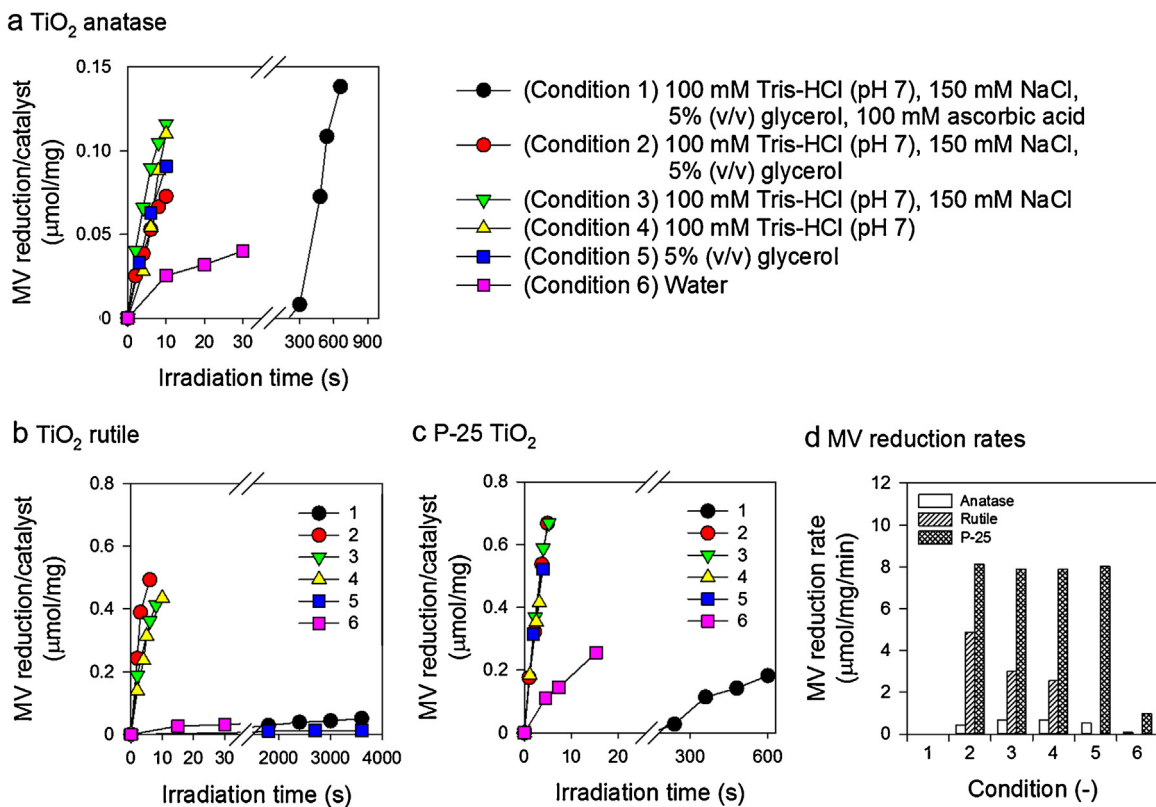


Fig. 2. Screening for efficient photocatalytic MV reduction under biocatalyst-friendly conditions. (a–c) Amounts of MV reduced using (a) anatase TiO₂, (b) rutile TiO₂, and (c) P-25 TiO₂ under various conditions. Components of the reaction solutions tested are indicated in the key legend. (d) MV reduction rates calculated based on the slopes measured in (a)–(c).

Inc., Japan)) through a gas sampler that was directly connected to the reaction system.

2.4. Measurement of AQY for photocatalytic MV reduction and hydrogen production

Except for an external light source, the amounts of MV reduced or hydrogen formed were measured using the same system described above. As light sources, 300 nm and 350 nm monochromatic light (MAX-302 with monochromatic filters, Asahi Spectra), and 420 nm and 470 nm light from an LED light source (OptoCode Corp.) were used. The number of incident photons was measured using a photodiode (S2281, Hamamatsu Photonics). The AQYs for photocatalytic MV reduction were represented as $AQY = 100 \times (\text{number of MV reduced}) / (\text{number of incident photons})^{-1}$. The AQYs for photocatalytic hydrogen production were represented as $AQY = 100 \times (2 \times \text{number of hydrogen molecules formed}) / (\text{number of incident photons})^{-1}$.

2.5. Hydrogen production by whole-cell biocatalyst

The whole-cell biocatalyst, recombinant *E. coli* BL21(DE3)/pEHydEA+pChyDFG, was prepared according to a previously described method [17]. A 2 mL of reaction solution containing 100 mM Tris-HCl (pH 7), 150 mM NaCl, 5% (v/v) glycerol, and 0.01 g-wet-cell of the whole-cell biocatalyst was prepared under anaerobic condition in 10 mL glass vials sealed with aluminum caps and rubber septa; headspace gas was replaced with nitrogen gas and the vials were pre-heated to 37 °C. Reaction was initiated by the addition of a solution of MV chemically reduced by an equimolar amount of sodium dithionite through the butyl rubber septum using a gas-tight syringe. The reaction was allowed

to proceed for 2 h at 37 °C and was then terminated by the addition of 10% (w/v) trichloroacetic acid. The amount of hydrogen formed in the headspace was detected using GC.

3. Results and discussion

3.1. Screening of reaction solution components appropriate for photocatalytic MV reduction

Components of the reaction solution for efficient photocatalytic MV reduction in a biocatalyst-friendly aqueous solution, such as buffer solution at natural pH, was screened using three different types of TiO₂ powders as the inorganic semiconductor; anatase TiO₂, rutile TiO₂, and P-25 TiO₂. Fig. 2a–d shows the amount of MV reduced under light irradiation using the TiO₂ powders under various biocatalyst-friendly conditions. Among the conditions tested, except for anatase TiO₂, the most efficient MV reduction was observed for condition 2, as shown in Fig. 2d. When ascorbic acid was included in the solution, photocatalytic MV reduction did not occur during the first several minutes, and the rates for MV reduction were lower than those under the other conditions (Fig. 2a–c).

Since the conduction band potential of anatase TiO₂ is more negative than that of rutile TiO₂ [23,24], the photocatalytic MV reduction activity of anatase TiO₂ was expected to be higher than that of rutile. However, under the conditions of 2, 3, and 4, rutile TiO₂ showed higher MV reduction activity as shown in Fig. 2. We measured the particle size and surface area of three types of TiO₂ powders used in this study (Table S1 in the Supporting Information). As shown in Table S1, the particle size and surface area of anatase TiO₂ were significantly different from those of rutile TiO₂ and P-25. Since the particle size of TiO₂ affects the photocatalytic activities [25–27], low MV reduction activity seems to be assigned

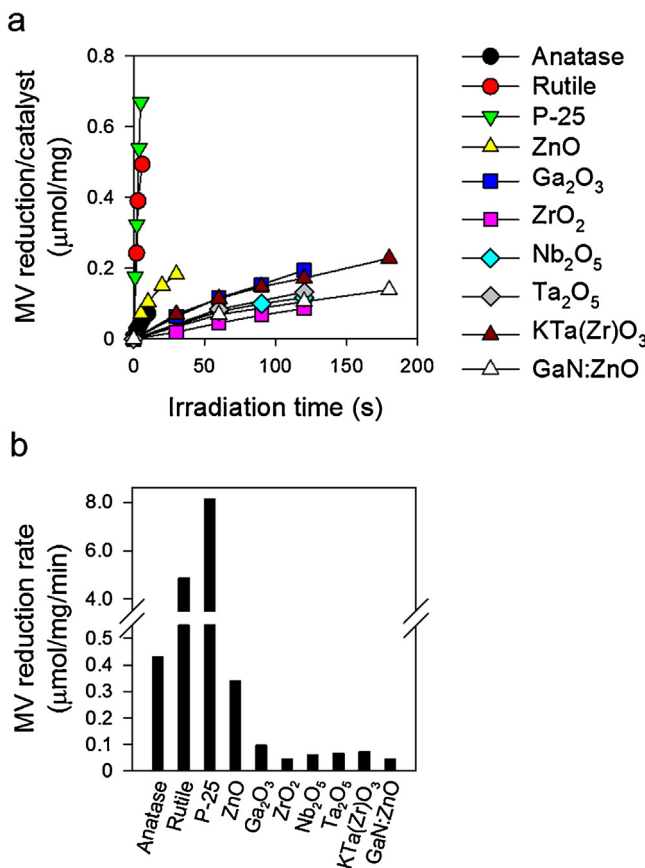


Fig. 3. Screening of inorganic semiconductors for photocatalytic MV reduction. (a) Amount of MV reduced using various semiconductors. (b) MV reduction rates calculated based on the slopes measured in (a). Reactions were performed in solutions of 100 mM Tris-HCl (pH 7), 150 mM NaCl, and 5% (v/v) glycerol (Condition 2).

to the large particle size and small surface area of anatase TiO₂ used in this experiment.

From these results, condition 2 (100 mM Tris-HCl (pH 7), 150 mM NaCl, and 5% (v/v) glycerol) was selected as the appropriate reaction solution for photocatalytic MV reduction.

3.2. Screening of inorganic semiconductors for photocatalytic MV reduction

Various inorganic semiconductor photocatalysts for photocatalytic MV reduction were investigated. Besides the three TiO₂ powders, ZrO₂, Nb₂O₅, Ta₂O₅, ZnO, KTa(Zr)O₃, Ga₂O₃, and GaN:ZnO were also tested in the photocatalytic MV reduction assay. Fig. 3a–b shows the amount of MV reduced using the common reaction solution (under condition 2: 100 mM Tris-HCl (pH 7), 150 mM NaCl, and 5% (v/v) glycerol) with various inorganic semiconductor photocatalysts. Fig. 3b shows that the inclusion of P-25 TiO₂ resulted in the highest MV reduction rate. The rate of MV reduction in the condition 2 reaction solution with P-25 TiO₂ reached 8.12 $\mu\text{mol}-(\text{MV reduced})\text{ mg}-(\text{P-25})^{-1}\text{ min}^{-1}$, which was 365 times higher than that with the previously-employed inorganic semiconductor photocatalyst (anatase TiO₂) and the reaction solution (100 mM Tris-HCl (pH 7), 150 mM NaCl, 5% (v/v) glycerol, and 100 mM ascorbic acid) [17]. There is only a limited amount of information regarding photocatalytic MV reduction using various inorganic semiconductors under biocatalyst-friendly conditions; therefore, the data presented here is expected to contribute to the development of MV-mediated inorganic-bio hybrid photocatalyst systems. It was concluded that

the mixture with 100 mM Tris-HCl (pH 7), 150 mM NaCl, and 5% (v/v) glycerol with P-25 TiO₂ was the most appropriate inorganic semiconductor photocatalyst for photocatalytic MV reduction (step 1).

3.3. Photocatalytic hydrogen production by combination of the enhanced MV reduction reaction and a biocatalyst

The enhanced photocatalytic MV reduction reaction (step 1) was combined with the photocatalytic hydrogen production reaction (step 2) using the whole-cell biocatalyst, recombinant *E. coli* BL21(DE3)/pEHydEA + pCHydFG [17]. Fig. 4 shows the amount of hydrogen formed from the reaction system under light irradiation. No oxygen was detected during either of the reactions. For reaction solution components of 100 mM Tris-HCl (pH 7) (Tris), 150 mM NaCl (NaCl), and 5% (v/v) glycerol (Gly) with P-25 TiO₂, the amount of hydrogen formed reached 0.95 mmol for a 2 h reaction, and stopped after the amount reached a maximum value of 0.99 mmol for a 3 h reaction period. We previously reported that the amount of hydrogen formed was 0.12 mmol for a 5 h reaction in a reaction solution of 100 mM Tris-HCl pH 7, 150 mM NaCl, 5% (v/v) glycerol, and 100 mM ascorbic acid (Tris100, NaCl, Gly, AA) [17]; therefore, enhancement of the step 1 reaction made a significant contribution to improvement of the hydrogen production.

We also checked the amount of hydrogen formed from the system in reaction solution components of 100 mM Tris-HCl (pH 7) (without NaCl and glycerol; condition 4 in Fig. 2) with P-25 TiO₂ (Fig. S1 in the Supporting Information). As shown in Fig. S1, the amount of hydrogen formed in the reaction solution (100 mM Tris-HCl (pH 7)) was approximately equal to that of hydrogen formed in the reaction solution (100 mM Tris-HCl (pH 7), 150 mM NaCl, 5% (v/v) glycerol). No effect of glycerol on the total amount of hydrogen formed was observed. This result suggested that Tris worked as the main electron donor in this system.

Tris is known as an efficient scavenger of hydroxyl radicals [28–30], which are formed by the water oxidation reaction with holes generated at the valence band (VB) of TiO₂ under light irradiation. When Tris is attacked by hydroxyl radicals, formaldehyde is produced from the reaction. Through the reaction, one mole of Tris can donate one mole of electron. In the reaction system in Fig. 4a, a maximum of 0.99 mmol of hydrogen was formed from 20 mL reaction solution containing 100 mM Tris-HCl (pH 7), 150 mM NaCl, and 5% (v/v) glycerol. If only Tris molecule worked as electron donor in the reaction system, the maximum number of electron from Tris in the 20-mL reaction system is 2 mmol, therefore, the theoretical amount of hydrogen formation is 1 mmol. On the other hand, formaldehyde is also known as an inhibitor of [FeFe]-hydrogenase [31], thus the accumulation of formaldehyde might affect the hydrogen formation of the inorganic-bio system. Therefore, the termination of hydrogen production is considered to be caused by the consumption of Tris in the reaction solution and toxicification of the cells or inhibition of [FeFe]-hydrogenase by formaldehyde formed from the reaction of Tris with hydroxyl radicals. The effect of the initial Tris concentration on the amount of hydrogen formed in the system was investigated. Fig. 4a and b shows that an increase in the initial Tris concentration causes an increase in the final amount of hydrogen formed, although the reaction rate and the ratio of the initial amount of Tris to the amount of hydrogen formed were decreased by an increase in the initial amount of Tris. These results suggest that Tris acts not only as a buffer reagent, but also as an efficient electron donor in the inorganic-bio hybrid system.

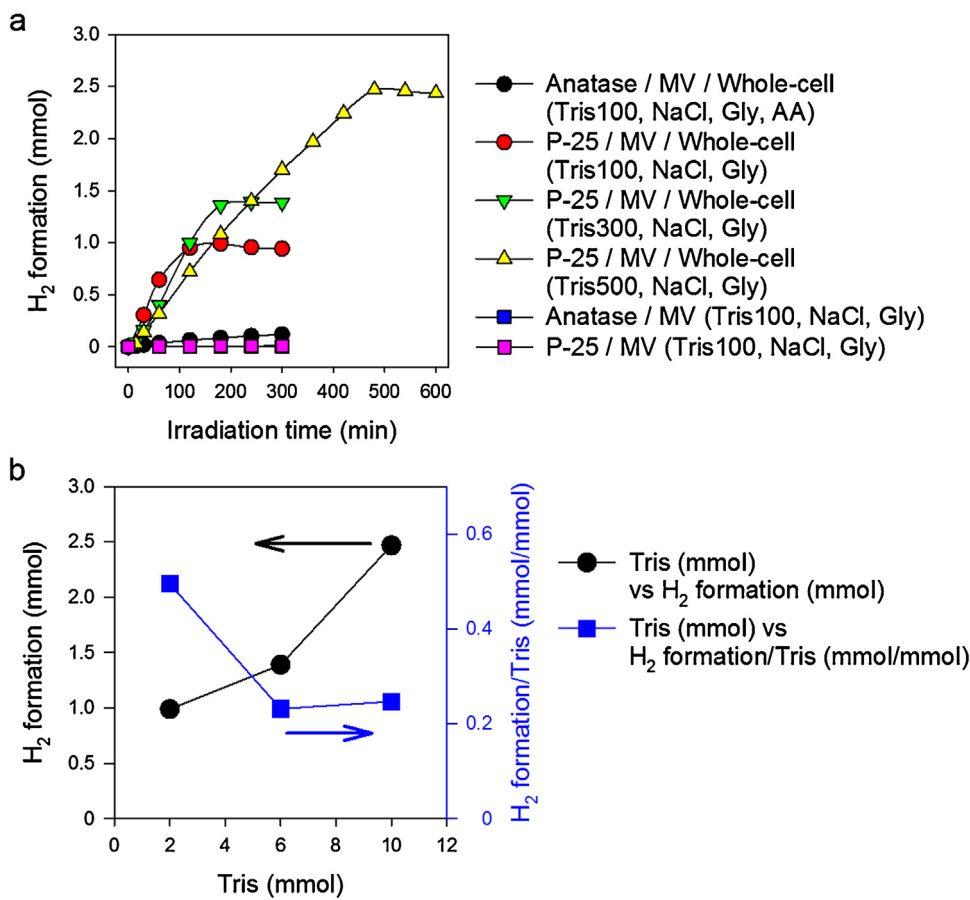


Fig. 4. Photocatalytic hydrogen production with the inorganic-bio hybrid system. (a) Amounts of hydrogen formed by the inorganic-bio hybrid system. The components of each reaction solution are indicated in parentheses: Tris-HCl at pH 7 (Tris), NaCl, 150 mM (NaCl), 5% (v/v) glycerol (Gly), 100 mM ascorbate (AA). The numbers indicated next to Tris represent the initial concentration (for example, Tris100 represents 100 mM Tris-HCl (pH 7)). (b) Effect of the initial amount of Tris on the final amount of hydrogen formed.

3.4. Apparent quantum yield (AQY) and efficiency for hydrogen production

To investigate the efficiency of the improved system for hydrogen production, the AQYs for the photocatalytic MV reduction (step 1), the efficiency for hydrogen production from chemically-reduced MV (step 2), and the AQYs for the photocatalytic hydrogen production (step 1 + step 2) were measured.

Fig. 5 shows the amounts of MV reduced under monochromatic light irradiation at 300 nm and 350 nm. These data were obtained from a mixture of the condition 2 reaction solution and P-25 TiO₂, without the whole-cell biocatalyst. The AQYs for photocatalytic MV reduction ($100 \times (\text{number of MV molecules reduced}) / (\text{number of incident photons})^{-1}$) were 60.8% and 52.2% under 300 and 350 nm light irradiation, respectively.

Fig. 6 shows the amounts of hydrogen formed from the reaction after 2 h with the whole-cell biocatalyst and various amounts of chemically-reduced MV. In the reaction, MV was reduced with equimolar amounts of sodium dithionite. The theoretical amount of hydrogen formed is half of the amount of reduced MV because two protons and two reduced MV molecules are used to form one molecule of hydrogen. When the initial amount of reduced MV was at least below 10 μmol (5 mM in 2 mL of reaction solution), almost 100% of reduced MV molecules was consumed by hydrogen formation with the whole-cell biocatalyst. These results suggest that chemically-reduced MV molecules are not utilized in other reactions, while the whole-cell biocatalyst contains native enzymes that utilize reduced MV as a substrate, besides heterologous [FeFe]-

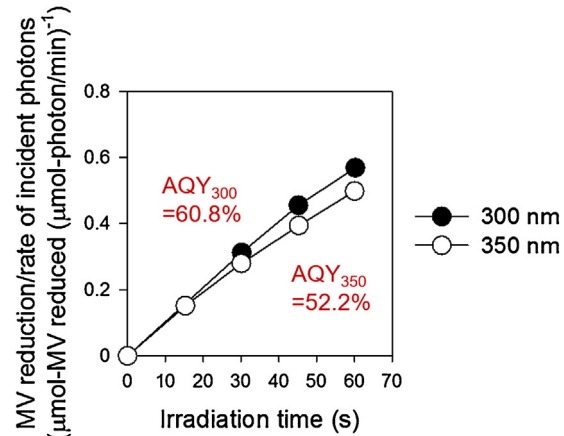


Fig. 5. Amounts of MV reduced under monochromatic light irradiation at 300 and 350 nm. The AQYs were calculated from the slopes measured for MV reduced and the incident photons. The amounts of incident photons were 4.72×10^{-7} and 7.94×10^{-7} mol-photon min⁻¹ at 300 and 350 nm, respectively.

hydrogenase. The hydrogen formation reaction is expected to occur easily because the redox potential of $\text{MV}^{2+}/\text{MV}^+$ ($E^{\circ'} = -0.44$ V vs. NHE, pH 7) [32] is closer to H^+/H_2 ($E^{\circ'} = -0.41$ V vs. NHE) than those of physiological redox chemicals or the electron transport chain that typically occur in *E. coli*, e.g., NAD^+/NADH ($E^{\circ'} = -0.32$ V vs. NHE) or ubiquinone/ubiquinol ($E^{\circ'} = +0.045$ V vs. NHE). Moreover, hydrogen formation is a dominant reaction in clostridial

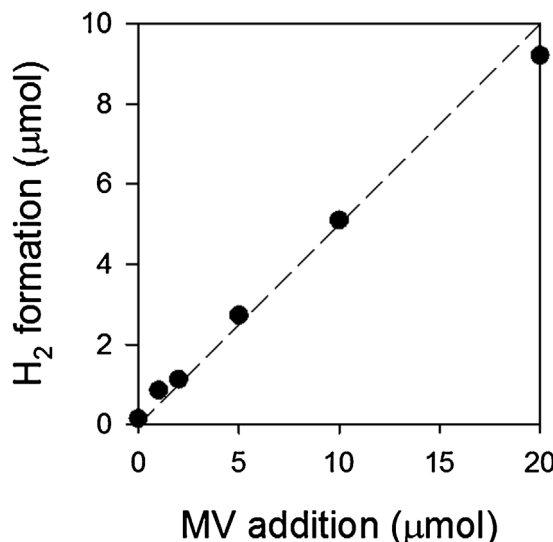


Fig. 6. Amounts of hydrogen formed using chemically reduced MV from the reaction of the whole-cell biocatalyst for 2 h. The dotted line indicates the theoretical amount of hydrogen produced from reduced MV.

[FeFe]-hydrogenase, and hydrogen molecules are not easily decomposed after formation by the whole-cell biocatalyst due to the lack of native [NiFe]-hydrogenase activity in *E. coli* BL21(DE3), which should contribute to the high efficiency. The results in Fig. 6 indicate that the hydrogen formation reaction (step 2) by the whole-cell biocatalyst was highly efficient.

Fig. 7 shows the amounts of hydrogen formed under various wavelengths of light irradiation. These data also show the entire performance of the inorganic-bio hybrid system for photocatalytic hydrogen production. The improved system is capable of producing hydrogen under light irradiation at 300, 350, and 420 nm; however, no hydrogen was detected under light irradiation at 470 nm. AQYs under light irradiation at 300, 350, and 420 nm were 26.4%, 31.2%, and 0.1%, respectively.

In addition, AQYs for photocatalytic MV reduction reaction (step 1) and hydrogen formation (step 1 + step 2) were plotted for discussing action spectrum of the system (Fig. S2 in the Supporting Information). As shown in Fig. S2a, AQY depends on the absorbance of P-25 TiO₂. Fig. S2b shows the emission spectrum of 420 nm LED light source and absorption spectrum of P-25 TiO₂. Since emission and absorption spectra are overlapped, hydrogen formation under 420 nm LED light irradiation is reasonable. The AQYs for hydrogen production at 300 nm and 350 nm (26.4% and 31.2%) were lower than those expected from the AQYs for step 1 MV reduction (60.8% and 52.2%) and the efficiency of step 2 hydrogen production (almost 100%). The AQYs for hydrogen production should be affected by light absorption and scattering by the whole-cell biocatalyst or by chemicals derived from the culture. In addition, the AQYs for hydrogen production could also be affected by the scattering of irradiated light on the reaction solution surface and aqueous droplets inside the reaction cells for photocatalytic hydrogen production. Hence, the AQYs for hydrogen production were lower than the AQYs for MV reduction. The amount of MV reduced under light irradiation at 350 nm should be much higher than that under light irradiation at 300 nm during photocatalytic hydrogen production, considering that the incident photons with 350 nm light (7.94×10^{-7} mol/min) were also higher than that with 300 nm light (4.72×10^{-7} mol/min). The higher amount of reduced MV may result in easier transfer of electrons to intracellular recombinant [FeFe]-hydrogenase in whole-cell catalyst, which results in higher hydrogen production. The higher AQY₃₅₀ (31.2%) than the AQY₃₀₀ (26.4%) for hydrogen production can be accounted for by the difference in the amount

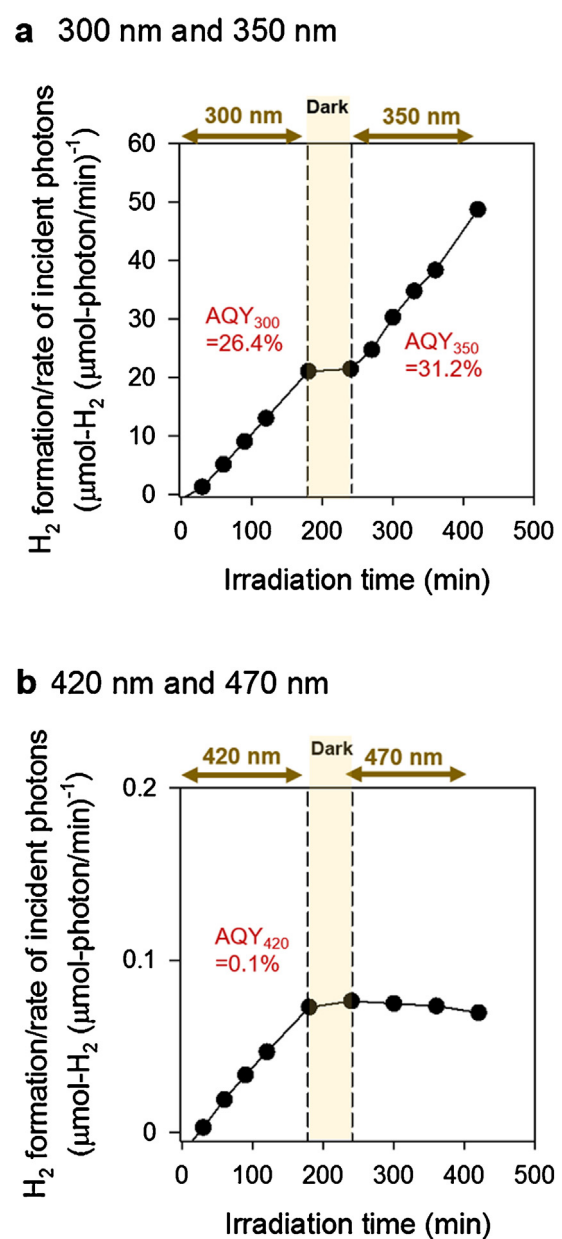


Fig. 7. Amounts of hydrogen formed under monochromatic light irradiation at 300, 350, 420 and 470 nm. The AQYs were calculated from the slopes measured for hydrogen formed and incident photons. The amounts of incident photons were 4.72×10^{-7} , 7.94×10^{-7} and 3.59×10^{-5} mol-photon min⁻¹ at 300, 350 and 420 nm, respectively.

of MV reduced during the reactions. It is noteworthy that the enhanced step 1 reaction caused an 88-fold increase in the AQY₃₀₀ (26.4%) compared with the AQY₃₀₀ for hydrogen production in the previously reported system (0.3%) [17].

4. Conclusions

In summary, the enhancement of photocatalytic MV reduction, as one part of the hydrogen production reaction with an inorganic-bio hybrid photocatalyst system, was investigated under biocatalyst-friendly conditions. Among the conditions tested, a reaction solution of 100 mM Tris-HCl (pH 7), 150 mM NaCl, and 5% (v/v) glycerol with P-25 TiO₂ showed the greatest enhancement of MV reduction. When these conditions were applied to the inorganic semiconductor/whole-cell biocatalyst hybrid system, the

photocatalytic hydrogen productivity was significantly improved. These results demonstrate that the newly developed inorganic-bio hybrid photocatalyst system, which is based on the combination of an inorganic semiconductor and a whole-cell biocatalyst, is a good candidate for clean hydrogen production. This system is expected to contribute to the development of a highly efficient, noble metal-free and clean photocatalytic hydrogen production system. Approaches for further improvement of the system, such as re-design of the reaction apparatus which enable the catalyst recovery and reuse, successive addition of electron donor, and control of pH and temperature are now under investigation, and these results will be reported in future.

Acknowledgement

This work was supported by the International Institute for Carbon-Neutral Energy Research (WPI-I2CNER), which was established by the World Premier International Research Center Initiative (WPI), MEXT, Japan.

Appendix A. Supplementary data

Supplementary data associated with this article can be found, in the online version, at <http://dx.doi.org/10.1016/j.apcatb.2017.04.015>.

References

- [1] R.E. Blankenship, D.M. Tiede, J. Barber, G.W. Brudvig, G. Fleming, M. Ghirardi, M.R. Gunner, W. Junge, D.M. Kramer, A. Melis, T.A. Moore, C.C. Moser, D.G. Nocera, A.J. Nozik, D.R. Ort, W.W. Parson, R.C. Prince, R.T. Sayre, Comparing photosynthetic and photovoltaic efficiencies and recognizing the potential for improvement, *Science* 332 (2011) 805–809.
- [2] D. Gust, T.A. Moore, A.L. Moore, Solar fuels via artificial photosynthesis, *Acc. Chem. Res.* 42 (2009) 1890–1898.
- [3] J. Barber, P.D. Tran, From natural to artificial photosynthesis, *J. R. Soc. Interface* 10 (2013) 20120984.
- [4] J.A. Macia-Agullo, A. Corma, H. Garcia, Photobiocatalysis: the power of combining photocatalysis and enzymes, *Chem. Eur. J.* 21 (2015) 10940–10959.
- [5] W. Lubitz, H. Ogata, O. Rüdiger, E. Reijerse, Hydrogenases, *Chem. Rev.* 114 (2014) 4081–4148.
- [6] P.M. Vignais, B. Billoud, Occurrence, classification, and biological function of hydrogenases: an overview, *Chem. Rev.* 107 (2007) 4206–4272.
- [7] P. Cuendet, K.K. Rao, M. Grätzel, D.O. Hall, Light induced H₂ evolution in a hydrogenase-TiO₂ particle system by direct electron transfer or via rhodium complexes, *Biochimia* 68 (1986) 217–221.
- [8] V.V. Nikandrov, M.A. Shlyk, N.A. Zorin, I.N. Gogotov, A.A. Krasnovsky, Efficient photoinduced electron-transfer from inorganic semiconductor TiO₂ to bacterial hydrogenase, *FEBS Lett.* 234 (1988) 111–114.
- [9] P. Pedroni, G.M. Mura, G. Galli, C. Pratesi, L. Serbolissa, G. Grandi, The hydrogenase from the hyperthermophilic archaeon *Pyrococcus furiosus*: from basic research to possible future applications, *Int. J. Hydrogen Energy* 21 (1996) 853–858.
- [10] E. Reisner, D.J. Powell, C. Cavazza, J.C. Fontecilla-Camps, F.A. Armstrong, Visible light-driven H₂ production by hydrogenases attached to dye-sensitized TiO₂ nanoparticles, *J. Am. Chem. Soc.* 131 (2009) 18457–18466.
- [11] C.Y. Lee, H.S. Park, J.C. Fontecilla-Camps, E. Reisner, Photoelectrochemical H₂ evolution with a hydrogenase immobilized on a TiO₂-protected silicon electrode, *Angew. Chem. Int. Ed.* 55 (2016) 5971–5974.
- [12] E. Reisner, J.C. Fontecilla-Camps, F.A. Armstrong, Catalytic electrochemistry of a [NiFeSe]-hydrogenase on TiO₂ and demonstration of its suitability for visible-light driven H₂ production, *Chem. Commun.* (2009) 550–552.
- [13] V. Pollio, S. Morra, S. Livraghi, F. Valetti, G. Gilardi, E. Gianneli, Electron transfer and H₂ evolution in hybrid systems based on [FeFe]-hydrogenase anchored on modified TiO₂, *Int. J. Hydrogen Energy* 41 (2016) 10547–10556.
- [14] K.A. Brown, S. Dayal, X. Ai, G. Rumbles, P.W. King, Controlled assembly of hydrogenase-CdTe nanocrystal hybrids for solar hydrogen production, *J. Am. Chem. Soc.* 132 (2010) 9672–9680.
- [15] K.A. Brown, M.B. Wilker, M. Boehm, G. Dukovic, P.W. King, Characterization of photochemical processes for H₂ production by CdS nanorod-[FeFe]-hydrogenase complexes, *J. Am. Chem. Soc.* 134 (2012) 5627–5636.
- [16] M.B. Wilker, K.E. Shinopoulos, K.A. Brown, D.W. Mulder, P.W. King, G. Dukovic, Electron transfer kinetics in CdS nanorod-[FeFe]-hydrogenase complexes and implications for photochemical H₂ generation, *J. Am. Chem. Soc.* 136 (2014) 4316–4324.
- [17] Y. Honda, H. Hagiwara, S. Ida, T. Ishihara, Application to photocatalytic H₂ production of a whole-cell reaction by recombinant *Escherichia coli* cells expressing [FeFe]-hydrogenase and maturases genes, *Angew. Chem. Int. Ed.* 55 (2016) 8045–8048.
- [18] H. Hagiwara, N. Ono, T. Inoue, H. Matsumoto, T. Ishihara, Dye-sensitizer effects on a Pt/KTa(Zr)₃ catalyst for the photocatalytic splitting of water, *Angew. Chem. Int. Ed.* 45 (2006) 1420–1422.
- [19] Y. Sakata, T. Nakagawa, Y. Nagamatsu, Y. Matsuda, R. Yasunaga, E. Nakao, H. Imamura, Photocatalytic properties of gallium oxides prepared by precipitation methods toward the overall splitting of H₂O, *J. Catal.* 310 (2014) 45–50.
- [20] K. Maeda, K. Domen, Solid solution of GaN and ZnO as a stable photocatalyst for overall water splitting under visible light, *Chem. Mater.* 22 (2010) 612–623.
- [21] H. Hagiwara, M. Nagatomo, C. Seto, S. Ida, T. Ishihara, Dye-modification effects on water splitting activity of GaN:ZnO photocatalyst, *J. Photochem. Photobiol. A: Chem.* 272 (2013) 41–48.
- [22] T. Watanabe, K. Honda, Measurement of the extinction coefficient of the methyl viologen cation radical and the efficiency of its forma, *J. Phys. Chem.* 86 (1982) 2617–2619.
- [23] L. Kavan, M. Grätzel, S.E. Gilbert, C. Klemenz, H.J. Scheel, Electrochemical and photoelectrochemical investigation of single-crystal anatase, *J. Am. Chem. Soc.* 118 (1996) 6716–6723.
- [24] D.O. Scanlon, C.W. Dunnill, J. Buckeridge, S.A. Shevlin, A.J. Logsdail, S.M. Woodley, C.R. Catlow, M.J. Powell, R.G. Palgrave, I.P. Parkin, G.W. Watson, T.W. Keal, P. Sherwood, A. Walsh, A.A. Sokol, Band alignment of rutile and anatase TiO₂, *Nat. Mater.* 12 (2013) 798–801.
- [25] C.B. Almquist, P. Biswas, Role of synthesis method and particle size of nanostructured TiO₂ on its photoactivity, *J. Catal.* 212 (2002) 145–156.
- [26] K. Kočí, L. Obalová, L. Matějová, D. Plachá, Z. Lacný, J. Jirkovský, O. Šolcová, Effect of TiO₂ particle size on the photocatalytic reduction of CO₂, *Appl. Catal. B: Environ.* 89 (2009) 494–502.
- [27] Y.F. Li, Z.P. Liu, Particle size, shape and activity for photocatalysis on titania anatase nanoparticles in aqueous surroundings, *J. Am. Chem. Soc.* 133 (2011) 15743–15752.
- [28] M. Hicks, J.M. Gebicki, Rate constants for reaction of hydroxyl radicals with Tris, Tricine and Hepes buffers, *FEBS Lett.* 199 (1986) 92–94.
- [29] V. Diesen, C.W. Dunnill, E. Osterberg, I.P. Parkin, M. Jonsson, Silver enhanced TiO₂ thin films: photocatalytic characterization using aqueous solutions of tris(hydroxymethyl)aminomethane, *Dalton Trans.* 43 (2014) 344–351.
- [30] M.S. Filipiak, A. Złocińska, P. Grzeskowiak, R. Lynch, M. Jönsson-Niedziolka, Tris(hydroxymethyl)aminomethane photooxidation on titania based photoanodes and its implication for photoelectrochemical biofuel cells, *J. Power Sources* 289 (2015) 17–21.
- [31] A.F. Wait, C. Brandmayr, S.T. Stripp, C. Cavazza, J.C. Fontecilla-Camps, T. Happe, F.A. Armstrong, Formaldehyde-a rapid and reversible inhibitor of hydrogen production by [FeFe]-hydrogenases, *J. Am. Chem. Soc.* 133 (2011) 1282–1285.
- [32] M.L. Fultz, R.A. Durst, Mediator compounds for the electrochemical study of biological redox systems – a compilation, *Anal. Chim. Acta* 140 (1982) 1–18.